ASTR-3415: Astrophysics Course Lecture Notes Section II

Dr. Donald G. Luttermoser East Tennessee State University

> Spring 2003 Version 1.2

Abstract
These class notes are designed for use of the instructor and students of the course ASTR-3415: Astrophysics. This is the Version 1.2 edition of these notes.

II. Stellar Spectra and the H-R Diagram

A. The Magnitude System

- 1. As shown in Equation (I-12), the magnitude of a light source is related to the logarithmic flux of that source. The magnitude system is defined such that 1st magnitude stars are approximately 100 times brighter than 6th magnitude stars (*i.e.*, the faintest that can typically be seen on a clear, moonless night).
- 2. It is often convenient to compare magnitudes of two different stars:

$$m_2 - m_1 = 2.5 \log \left(\frac{f_1}{f_2}\right)$$
 (II-1)

- 3. Magnitudes that are measured from Earth (actually at the top of the atmosphere) are called **apparent magnitudes** (m).
- 4. The absolute magnitude (M) is the magnitude that a source would have if at a distance d of 10 parsecs (see §IX). It is related to the apparent magnitude (ignoring interstellar absorption) by

$$m - M = 5 \log \left(\frac{d}{10 \text{ pc}}\right) = 5 \log d - 5$$
. (II-2)

- 5. Often, a magnitude is measured in a certain filter (say the V band filter). In these cases, the magnitudes are listed with a subscript defining the filter $(e.g., M_V)$.
- 6. The magnitude integrated across the entire spectrum is called the **bolometric magnitude**, M_{bol} , of the object.
 - a) M_{bol} is related to M_V with

$$M_{\rm bol} = M_V + BC , \qquad (II-3)$$

where BC is called the **bolometric correction**.

b) You can relate M_{bol} to the luminosity of a star with

$$M_{\text{bol}} = 4.72 - 2.5 \log(L/L_{\odot})$$
, (II-4)

where 4.72 is the bolometric magnitude of the Sun and $L_{\odot}(=3.8268 \times 10^{33} \text{ erg/s})$ is the solar luminosity.

c) Finally, you can determine the luminosity of a star through the Stefan-Boltzmann Law (Eq. I-16) and Eq. I-10:

$$L = 4\pi \,\sigma \,R^2 \,T_{\text{eff}}^4 \,, \tag{II-5}$$

where R is the radius of the star and T_{eff} is the effective temperature of the star.

- i) The effective temperature of a star is the temperature as derived from the Stefan-Boltzmann Law (Eq. I-16).
- ii) Typically it corresponds to the temperature of the atmospheric depth where the emergent continuum arises near λ_{max} .

B. Classification Schemes

- 1. Spectral Classification
 - a) The first large-scale classification of stellar spectra was undertaken by Mrs. W.P. Fleming, Antonia Maury, and Annie Jump Cannon in the 1920's at Harvard College Observatory and became known as the Henry Draper (HD) catalog.
 - i) Over 400,000 stars were classified.
 - ii) Stars were grouped by hydrogen (Balmer) line strengths with designations A-S.

- iii) Classes C, D, E, H, I, J, L, P, and Q were dropped for one reason or another or merged into other classes (see Jaschek and Jaschek 1987, *The Classification of Stars*, Cambridge Press).
- iv) The R and N stellar classifications corresponded to carbon stars and now have been merged into one classification designated C (although not the same as the original C stars, which were spectroscopic binaries). Many people however still use the R and N classification (including me) to describe carbon stars. R stars are the hotter of the two and correspond to the oxygen-rich K stars in temperature. The N-type carbon stars correspond to the coolest oxygen-rich M stars in temperature. Carbon stars differ from oxygen-rich stars in that there visual spectrum is dominated by carbon molecule (i.e., C₂, CN, and CH) absorption bands.
- v) S stars are another special class similar in temperature to late K and M stars. The S star's spectrum is dominated by LaO, VO, and ZrO molecular bands.
- b) Groups were rearranged from the hottest (called early-type stars) to the coolest (called late-type stars) and 10 subdivisions for each group introduced. Each "spectral type" is determined by various line strengths and line ratios (see Figure II-1). A brief overview is displayed in Table II-1. A more complete description can be found in Jaschek and Jaschek (1987) and Kaler (1989, Stars and

 ${\bf Table~II-1:~Spectral~Classifications}$

Spectral	Special		
Type	Classes	Temperatures	Spectral Characteristics
O 5–9		50,000-28,000 K	He II lines.
"	${f f}$,,	He II ($\lambda 4686$) & N III ($\lambda \lambda 4630-34$) in emission.
>>	e	"	He II & N III in absorption, H in emission.
"	WC5–WC8	"	Wolf-Rayet (carbon sequence), O-star spectrum,
			wide emission lines.
>>	WN6-WN8	"	Wolf-Rayet (nitrogen sequence), O-star spectrum,
			wide emission lines.
В 0-9		28,000-9,900 K	He I lines, H lines strengthen.
"	e	"	He I, H emission lines.
"	p	"	B-star spectrum; Si II, Mn II, Cr II, Eu II, Sr II
			are strong.
A 0-9		9,900-7,400 K	H lines strong, Ca II H & K strengthen toward
			later type.
"	p	"	A-star spectrum; Si II, Mn II, Cr II, Eu II, Sr II
			are strong.
"	m	"	A-star spectrum + Fe lines unusually strong.
F 0-9		7,400-6,000 K	Metals, H lines weaken, Ca II strengthen —
			emission "bumps" appear in H & K line cores at F4.
G 0–9		6,000–4,900 K	Ca II very strong, Na I D line strengthens, metals.
>>	${ m Ba}$	_	(G2-K4) spectrum, Ba II ($\lambda 4554$) very strong.
"	СН	_	(G5-K5) spectrum, CH band ($\lambda 4300$) very strong.
K 0-7		4,900-3,900 K	Ca II strong, Ca I ($\lambda 4227$) strengthens, molecular
			bands form.
M 0-10	<u> </u>	3,900-2,500 K	TiO bands dominate visual spectrum, neutral metals
			very strong.
S 0-9	_	4,200–2,500 K	(K5-M) type stars except ZrO, VO, & LaO molecular
			bands strong.
R 0-9		4,800–3,200 K	C_2 , CN, CH strong, = $C0$ -C5 classification.
N 0-7		3,200–2,500 K	C ₂ , CN, CH strong, strong violet flux depression,
			=C6-C9 classification.

Their Spectra, Cambridge Press).

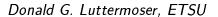
c) Later it was found by Saha, that the sequence of spectral types from hottest to coolest stars should follow:

OBAFGKM(RNS)

- i) Classes R, N, and S are special as described above.
- ii) The weakness of the H lines in O stars is due to most of the hydrogen being completely ionized.
- iii) The weakness of the H lines in M stars is due to their cool atmospheres, most of the electrons are in the ground state, with virtually none in the 2nd level where the Balmer lines arise (see below).

2. Luminosity Classification

- a) Later you will see that particle collisions are one cause of line broadening. Since collisional rates are a function of density and density depends on the surface gravity of a star; bigger, lower gravity stars will tend to have sharper lines than high gravity stars for a given spectral type.
 - i) Luminosity depends both on the radius and temperature of a star.
 - ii) NOTE: Don't be fooled in thinking that a broad line automatically implies a dwarf star there are other opacity sources (and velocity fields) that can broaden a line. A broader line "for the same spectral type" generally implies higher gravity.
- b) Table II-2 displays the luminosity classification system.



II-6

Figure II–1: Synthetic spectra of the hottest to coolest main sequence stars (see §II-H), plotted from 2000 Å (near UV) to 10,000 Å (near IR). Note the strong H-lines in the A star and the strong molecular bands (due to TiO) in the M stars. Also note the redward shifting of λ_{max} as the stars get progressively cooler.

Luminosity		Abso	lute Vi	sual Mag
Class	Type	В0	F0	M0
Ia	Luminous supergiants	-6.7	-8.2	-7.5
Ib	Less luminous supergiants	-6.1	-4.7	-4.6
II	Bright giants	-5.4	-2.3	-2.3
III	Normal giants	-5.0	1.2	-0.4
IV	Subgiants	-4.7	2.0	
V	Main sequence (dwarfs)	-4.1	2.6	9.0
sd (VI)	Subdwarfs (pop II dwarfs)			10.0
wd (VII)	White dwarfs	10.2	12.9	

Table II–2: Luminosity Classifications

- 3. The Morgan-Keenan (M-K) classification of a star is simply the spectral type along with the luminosity class and defines a star's location on an H-R diagram (i.e., the Sun is a G2 V star, α Boo a K1 III star, see below).
- 4. The Wilson-Bappu effect is a very powerful technique in determining a star's absolute magnitude (M_V) , which is related to a star's luminosity by Eq. (II-4).
 - a) Figure II-2 displays the Ca II K line at $\lambda 3934$ of α Boo as observed through the McMath-Pierce Solar Telescope on Kitt Peak. Note the emission bumps near line center (labeled K_2) these bumps indicate the existence of a chromosphere for this star (more to come).
 - **b)** The Wilson-Bappu effect has the following functional form:

$$M_V = -14.9 \log \omega + 27.6 \quad (\pm 0^m.5),$$
 (II-6)

where ω is the separation (in units of km/s) between the K_1 features (see Figure II-2). Obviously this empirical relation can on be used for stars with chromospheres.

Figure II–2: Ca II K line of Arcturus (K1 III). The chromospheric emission bumps are indicated with K_2 labels.

- c) There is some debate as to why the Wilson-Bappu effect works. Athay and Skumanich (1968, Astrophys. Journ., 152, 141) proposed that it is the result of turbulent motions in the chromosphere (turbulence also plays a role in line broadening), although it is not obvious how the photospheric flux (i.e., M_V) influences turbulent motions in the chromosphere (note: these regions in a stellar atmosphere will be defined in the next section on the solar atmosphere), especially since this relation hold for all luminosity classes.
- d) Ayres, Linsky, and Shine (1975, Astrophys. Journ., 195, L121) have proposed what I consider to be the correct explanation for the validity of this effect: More luminous stars have more mass above their photospheres than less luminous stars, and hence, the optical depth is greater at the temperature minimum (connecting point between

Name	λ (Å)	Origin
A	7594	O_2 (terrestrial oxygen)
a	7165	H ₂ O (terrestrial water vapor)
В	6867	O_2 (terrestrial oxygen)
С	6563	$H\alpha$ (3/2 transition)
D	5890, 5896	Na I (resonance lines, D-lines)
\mathbf{E}	5270	Fe I
b	5167, 5173, 5184	Mg I (b-lines)
F	4861	${ m H}eta~(4/2~{ m transition})$
d^{\dagger}	4384	Fe I
G	4300	CH band
g^{\dagger}	4227	Ca I (resonance line)
h^{\dagger}	4102	$H\delta$ (6/2 transition)
Н	3968	Ca II (resonance line)
K^{\dagger}	3934	Ca II (resonance line)

Table II-3: The Fraunhofer Lines

† Not an original Fraunhofer designation: added later.

the photosphere and chromosphere). Since the K_1 feature is formed at T_{\min} , it will be broader in more luminous stars due to the higher opacity in Ca II at T_{\min} .

C. Stellar Spectra

- 1. Each star of a certain MK class has a characteristic spectrum associated with it. Besides the relative strength of certain lines and the appearance and disappearance of various spectral features, the shape of the underlying continuum changes as well.
- 2. The spectrum of the Sun was first mapped by Joseph von Fraunhofer in the early 1800s. He observed over 500 absorptions and assigned letters to the most prominent of them proceeding from red to blue, long before any chemical origin could be known. Table II-3 lists the most prominent of these lines and gives their chemical origin.

- 3. Whereas Figure II-1 showed *synthetic* spectra for various spectral classes, Figures II-3 and II-4 display visual *stellar* spectra of various MK classes for your reference. Note the location of λ_{max} , the strength of the Balmer lines, and the appearance of molecular features in cooler stars.
- 4. Often in stellar spectra, one may see very sharp lines superimposed on the broader stellar lines. These are interstellar lines, whose strength depends upon the amount of material between the Earth and the star. Figure II-5 displays a spectrum of the O5 star θ^1 Ori (the brightest Trapezium star in M42) in the Ca II H & K region. An O5 star is too hot to display Ca II, yet 2 sharp Ca II lines are seen at 3934 Å and 3968 Å and are due to the M42 nebula itself.
- **5**. The absorption lines in the visual spectrum of a star generally yield information on the stellar photosphere. Radio observations yield data on stellar coronae and ionized winds. The infrared (IR) region is useful in the study of dusty environments around stars (i.e., circumstellar shells around late-type giants and supergiants, stellar nurseries). The ultraviolet (UV) gives valuable information on stellar chromospheres (especially the near-UV, 1216 Å (Lyman α) - 3200 Å, where lines such as Mg II h and k at 2795.523 Å and 2802.698 Å, respectively, are used to semiempirically model chromospheres) and transition regions (i.e., the C IV lines at 1548.195 Å and 1550.768 Å). The far-UV (FUV: 912 Å (Lyman limit) – 1216 Å), the extreme-UV (EUV: 100 Å - 912 Å), and X-ray (1 Å - 100 Å) regions are dominated by highly ionized lines, which makes these regions useful for the study of high temperature $(T \ge 10^6 K)$ regimes like stellar coronae and accretion disks.

Figure II-3: Sample of stellar spectra for various early-type MK classes.

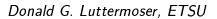
Figure II-4: Sample of stellar spectra for various late-type MK classes.

Figure II–5: θ^1 Ori spectrum in the Ca II H & K spectral region.

- a) Figure II-6 shows a low-resolution (\sim 6Å) *IUE* spectrum of the N-type carbon star TX Psc with some prominent chromospheric emission lines labeled.
- b) Figure II-7 displays a synthetic spectrum of a mass-exchange binary system AR Lac in the X-ray and EUV region. The strong emission lines are from highly ionized metals.
- c) One must be careful when discussing wavelengths of various lines in the UV, since some authors prefer to work with vacuum wavelengths (typically for $\lambda < 2000$ Å) and others with air wavelengths ($\lambda > 2000$ Å). A shift in wavelength occurs in air due to the reduced speed of light. The air wavelength relates to the vacuum wavelength by

$$\lambda_{
m air} = rac{\lambda_{
m vac}}{n_{
m air}} \; , \qquad \qquad {
m (II-7)}$$

where the index of refraction $n_{\rm air}$ is a function of wavenum-



II-14

Figure II–6: Low resolution IUE spectrum of TX Psc.

Figure II–7: Synthetic spectrum of the mass-exchange binary system AR Lac.

ber $(\overline{\nu} = 1/\lambda_{\text{vac}})$ and expressed by

$$n_{\rm air} = 1 + 6.4328 \times 10^{-5} + \frac{2,949,810}{1.46 \times 10^{10} - \overline{\nu}^2} + \frac{25,540}{4.1 \times 10^9 - \overline{\nu}^2} \,. \label{eq:nair}$$
 (II-8)

6. Line strengths are often expressed in terms of equivalent widths (W_{λ}) , which is defined by

$$W_{\lambda} = \int_{0}^{\infty} \left(1 - \frac{F_{\lambda}}{F_{cont}} \right) d\lambda , \qquad (II-9)$$

where F_{cont} is the continuum flux at line center. W_{λ} is usually expressed in units of mÅ and describes the width of a box whose area is the as the area between the continuum and the line profile (see Figure 9.18 in Carroll & Ostlie).

- 7. The amount of information contained in a spectrum depends upon its spectral resolution the ability to separate two closely spaced lines. **Spectral resolution** $(\delta\lambda)$ is usually expressed in units of Å and is related to the **resolving power** by $R = \lambda/\delta\lambda$. Many times the resolution of a spectrum is given in terms of **linear (plate) dispersion** $(d\lambda/dx)$, in units of Å/mm). A rule of thumb is that a resolving power of $20,000 \approx 4$ Å/mm.
- 8. Chemical abundances are determined from line strengths. Typically, an elemental abundance is tabulated in the form of [X/H],

$$[X/H] \equiv \log[n(X)/n(H)]_{\star} - \log[n(X)/n(H)]_{\odot}, \qquad (II-10)$$

where X is the element in question. To make matters more confusing, elemental abundance is sometimes scaled to the hydrogen abundance, with the logarithm of the hydrogen abundance normalized to 12.00. For instance, the solar abundance for sodium in this system is 6.33. This means that the actual abundance, $\alpha = n(X)/n(H)$, is 2.14×10^{-6} (log $\alpha = 6.33 - 12.00 =$

-5.67). In the ATLAS stellar atmosphere code, the abundance is tabulated with respect to the total number density and <u>not</u> the hydrogen density. One can adjust from one to the other by realizing that n(H)/n(total) = 0.908 in the Sun. Except for the peculiar hydrogen deficient stars, it is always assumed that stellar hydrogen abundance is equivalent to the solar value.

D. The Spectrum of Hydrogen

1. Rydberg (1890), Ritz (1908), Planck (1910), and Bohr (1913) were all responsible for developing the theory of the spectrum of the H atom. A transition in an hydrogen-like atom/ion from an upper level m to a lower level n will radiate a photon at frequency

$$\nu_{mn} = c \, R_A \, Z^2 \, \left(\frac{1}{n^2} - \frac{1}{m^2} \right),$$
(II-11)

where the velocity of light, $c = 2.997925 \times 10^{10}$ cm/s, Z is the effective charge of the nucleus ($Z_H = 1, Z_{He} = 2$, etc.), and the atomic Rydberg constant, R_A , is given by

$$R_A = R_\infty \left(1 + \frac{m_e}{M_A} \right)^{-1}. \tag{II-12}$$

a) The Rydberg constant for an infinite mass is

$$R_{\infty} = \frac{2\pi^2 m_e e^4}{c h^3} = 109,737.31 \text{ cm}^{-1},$$
 (II-13)

where $e=4.80325\times 10^{-10}$ esu is the electron charge in cgs units.

b) In atomic mass units (amu), the electron mass is $m_e = 5.48597 \times 10^{-4}$ amu whereas the atomic mass, M_A , can be found on the periodic table I passed out earlier (see also Table II-4).

Atom	Atomic Mass, M_A	Rydberg Constant, R_A	
	(amu)	$({ m cm}^{-1})$	
Hydrogen, ¹ H	1.007825	109,677.6	
Helium, ⁴ He	4.002603	109,722.3	
Carbon, ¹² C	12.000000	109,732.3	
Nitrogen, ¹⁴ N	14.003074	$109{,}733.0$	
Oxygen, ¹⁶ O	15.994915	109,733.5	
Neon, ²⁰ Ne	19.992440	109,734.3	

Table II-4: Atomic Masses and Rydberg Constants

c) Eq. (II-11) can also be expressed in wavelengths (vacuum) by the following

$$\frac{1}{\lambda_{mn}} = R_A Z^2 \left(\frac{1}{n^2} - \frac{1}{m^2} \right).$$
 (II-14)

- Lines that originate from the same level in a hydrogen-like atom/ion are said to belong to the same series (see Figure I-6). Transitions out of (or into) the ground state (n = 1) are lines of the Lyman series, n = 2 corresponds to the Balmer series, and n = 3, the Paschen series.
- 3. For each series, the transition with the longest wavelength is called the alpha (α) transition, the next blueward line from α is the β line followed by the γ line, etc.
 - a) Lyman α is the $1 \leftrightarrow 2$ transition, Lyman β is the $1 \leftrightarrow 3$ transition, Lyman γ is the $1 \leftrightarrow 4$ transition, etc.
 - **b)** Balmer or $H\alpha$ is the $2 \leftrightarrow 3$ transition, $H\beta$ is the $2 \leftrightarrow 4$ transition, $H\gamma$ is the $2 \leftrightarrow 5$ transition, etc.

E. Lines from Other Atoms and Molecules.

- 1. Except for helium, line transitions are difficult to determine semiclassically or quantum mechanically. Their characteristics (i.e., wavelengths, energy levels, oscillator strengths, etc.) are often determined experimentally.
- 2. Wavelengths for all atomic species has been tabulated by Dr. Charlotte Moore in her famed Multiplet Tables of Atomic Species. Meanwhile, Dr. Robert Kurucz of Harvard University has an electronic version of a atomic and diatomic molecular lines that contains over 42 million lines! The code ATLAS, which you will be using later in the course, uses this Kurucz line list.
- **3.** To properly model atomic lines, one needs to know the shape of the **line profile**. These profiles typically have a *Gaussian*, *Lorentzian*, or *Voigt* (combination of the previous two) profile (see below).
- 4. Molecular lines outnumber atomic lines in the spectra of cool stars.
 - a) Each individual line is narrow with a Gaussian profile.
 - b) These narrow lines appear in large groupings in spectra called **molecular bands**. Each band has a sharp **band** head that marks the beginning wavelength location of the band.
 - c) Molecules composed of 2 atoms (e.g., CO, OH, CN, etc.) are called **diatomic molecules**.
 - d) If they contain more than 2 atoms (e.g., H_2O , CO_2 , HCN, etc.), they are typically called **polyatomic molecules**.

F. Level Thickness and Probabilities.

- 1. The equation of radiative transfer is an equation specifying the manner in which a beam of radiation interacts with gas consisting on an ensemble of atoms.
 - a) Consequently, we introduce the quantity ϕ_{ν} , which attempts to detail the manner in which a photon is absorbed by the gas.
 - b) We must include not just one atom but the entire ensemble \Longrightarrow we define $n_i\phi_{\nu}$ to be the probability of a photon of frequency ν traveling in the direction (*i.e.*, solid angle) Ω being absorbed by an ensemble n_i atoms with an bound electron in the lower level.
 - c) Correspondingly we define $n_u\psi_{\nu}$ to be the probability of an ensemble of n_u atoms in the excited state emitting a photon of frequency ν and direction Ω as result of spontaneous and stimulated de-excitation (note that the ψ_{ν} profile is the same for stimulated and spontaneous emission).
 - d) In this class, we will assume that $\psi_{\nu} = \phi_{\nu}$ (i.e., the emission profile = the absorption profile) \Longrightarrow complete redistribution of the photons in the line.
- 2. Each excited energy state has a natural finite width associated with it in accordance to the Heisenberg Uncertainty Principle $(\Delta E \Delta t \geq \hbar)$, where Δt is the probable time that an e^- stays in an excited state. Note that the ground state has an infinite lifetime and as such is infinitely sharp $(i.e., \Delta E = 0)$.

Figure II-8: The broadening of excited states in relation to the broadening of lines.

- 3. Besides this natural broadening, states can be broadened further by interactions with other other particles \implies collisional broadening.
 - a) The line profile ϕ_{ν} is then determined by a convolution of the probability distributions of the 2 states involved in the transition (see Figure II-8).
 - b) Since we are dealing with an ensemble of particles, a line profile can be broadened further by Doppler motions of the individual atoms in the ensemble which result from the thermal effects.
 - c) Microturbulent velocities ($\xi \ll c_s$) of the gas exist as well and are added with the thermal motions of the gas.

- 4. Additional broadenings on the *macroscopic* level must also be taken into account when analyzing spectra.
 - a) The rotation of the emitting object can also broaden a line (as well as other macroscopic velocities), for high rotational velocity stars, this can sometimes dominate the line broadening.
 - b) Finally, the instrument for which you observe the object broadens the line \Longrightarrow the instrument profile, generally Gaussian in shape. It must be determined during an observation (usually with a comparison lamp spectrum with "infinitely" sharp lines) and the spectrum then "deconvolved" of the instrument profile \Longrightarrow or in the other direction, a synthetic spectrum must be "convolved" with the instrument profile before a comparison can be made with the observation.

G. Line Broadening.

1. The line absorption coefficient can be expressed in terms of frequency (Eq. I-27) or in delta-wavelength with

$$\Delta \lambda = \lambda - \lambda_{\circ} = \lambda - \frac{c}{\nu_{\ell u}} \,, \tag{II-15}$$

where λ_{\circ} is called the line center (even in cases of grossly asymmetric profiles) and $\nu_{\ell u}$ is the frequency difference between the undisturbed states ℓ and u.

a) The absorption profile is normalized to

$$\int_{-\infty}^{\infty} \phi(\Delta \lambda) \, d\Delta \lambda = 1 \ . \tag{II-16}$$

b) Since $\phi(\nu) d\nu = -\phi(\Delta \lambda) d\Delta \lambda$, we can rewrite the absorption coefficient of Eq. I-27, without stimulated emission, as (e.g., Eq. I-28)

$$\kappa_{\Delta\lambda}(line) = n_i \alpha_{\lambda} = n_i f_{ij} \frac{\pi e^2 \lambda_o^2}{m_e c^2} \phi(\Delta\lambda) .$$
(II-17)

c) If the line is broadened by two mechanisms with $\phi_1(\Delta \lambda)$ and $\phi_2(\Delta \lambda)$ which are not correlated with one another, $\phi(\Delta \lambda)$ is obtained as the convolution integral

$$\phi(\Delta \lambda) = \int_{-\infty}^{\infty} \phi_1(\Delta \lambda - x) \, \phi_2(x) \, dx \,. \tag{II-18}$$

- 2. There are 3 types of line profiles that we will discuss: Gauss, Lorentz, and Voigt profiles.
 - a) The Gauss profile with peak value $1/(\sqrt{\pi}\Delta\lambda_{\rm G})$ and fullwidth at half-maximum (FWHM) $\Delta\lambda_{\rm G}$ (also called the half-width) is given by

$$\phi(\Delta \lambda) = \frac{1}{\sqrt{\pi} \Delta \lambda_{G}} \exp\left(\frac{-\Delta \lambda^{2}}{\Delta \lambda_{G}^{2}}\right) . \tag{II-19}$$

Convolution of 2 Gauss profiles with $\Delta \lambda_{G1}$ and $\Delta \lambda_{G2}$ (and same λ_{\circ}) yields another Gauss profile with $\Delta \lambda_{G}^{2} = \Delta \lambda_{G1}^{2} + \Delta \lambda_{G2}^{2}$.

b) The Lorentz (dispersion, damping) profile with peak value $2/(\pi\Delta\lambda_{\rm L})$ and FWHM $\Delta\lambda_{\rm L}$ is given by

$$\phi(\Delta \lambda) = \frac{\Delta \lambda_{\rm L}}{2\pi} \frac{1}{\Delta \lambda^2 + \Delta \lambda_{\rm r}^2 / 4} , \qquad (\text{II-20})$$

with

$$\Delta \lambda_{\rm L} = \frac{\lambda_{\rm o}}{\omega_{\rm o}} \gamma = \left(\frac{\lambda_{\rm o}^2}{2\pi c}\right) \gamma , \qquad (\text{II-21})$$

where γ is the damping constant (note that this γ is in terms of ν -space — even though it is used in λ -space here). Convolution of 2 Lorentz profiles with γ_1 and γ_2 (and same λ_{\circ}) yields another Lorentz profile with $\gamma = \gamma_1 + \gamma_2$.

c) Convolution of a Gaussian and Lorentzian (with same λ_{\circ}) yields a **Voigt profile**:

$$\phi(\Delta \lambda) = \frac{1}{\sqrt{\pi} \Delta \lambda_{G}} H(a, v) , \qquad (II-22)$$

where the Voigt function is defined by

$$H(a,v) = \frac{a}{\pi} \int_{-\infty}^{\infty} \frac{e^{-y^2}}{a^2 + (v - y)^2} dy$$
$$= \frac{1}{\sqrt{\pi}} \int_{0}^{\infty} e^{-ax - x^2/4} \cos(vx) dx , \text{ (II-23)}$$

$$a = \frac{\gamma}{2\Delta\omega_{\rm G}} = \frac{\gamma}{(4\pi c/\lambda_{\rm o}^2)\Delta\lambda_{\rm G}} = \frac{\Delta\lambda_{\rm L}}{2\Delta\lambda_{\rm G}} , \qquad (\text{II-24})$$

$$v = \frac{\Delta \lambda}{\Delta \lambda_{\rm G}} \ . \tag{II-25}$$

A Gauss and a Lorentz profile are recovered from the Voigt profile in the limit $a \to 0$ and $a \to \infty$, respectively. The normalization and the limits of the Voigt function H(a, v) are

$$\int_{-\infty}^{\infty} H(a, v) \, dv = \sqrt{\pi} \,, \tag{II-26}$$

$$\lim_{a \to 0} H(a, v) = e^{-v^2} , \qquad (II-27)$$

$$\lim_{a \to \infty} H(a, v) = \frac{a}{\sqrt{\pi}(a^2 + v^2)}. \quad (\text{II-28})$$

If $a \ll 1$, the following simple approximation may be used for coarse studies:

$$H(a, v) \simeq e^{-v^2}$$
 (for $v < 1, a \ll 1$) (II-29)

$$H(a,v) \simeq e^{-v^2} + \frac{a}{\sqrt{\pi} v^2}$$
 (for $v > 1, a \ll 1$). (II-30)

A fast computer routine which is accurate to $\sim < 0.1\%$ over the whole (a, v)-plane can be written from the following equations:

$$H(a,v) \simeq e^{-v^{2}} + av^{-2} \sum_{j=0}^{6} c_{j}v^{-2j} + a^{2}(1 - 2v^{2})e^{-v^{2}}$$

$$(\text{for } a \leq 10^{-3}, \ v \geq 2.5), \qquad (\text{II-31})$$

$$H(a,v) \simeq \Re\left[\frac{\sum_{j=0}^{6} a_{j}\zeta^{j}}{\left(\zeta^{2} + \sum_{j=0}^{6} b_{j}\zeta^{j}\right)}\right]$$

$$(\text{otherwise}), \qquad (\text{II-32})$$

j	c_{j}	a_{j}	b_j
0	0.5641641	122.607931777104326	122.607931773875350
1	0.8718681	214.382388694706425	352.730625110963558
2	1.474395	181.928533092181549	457.334478783897737
3	-19.57862	93.155580458138441	348.703917719495792
4	802.4513	30.180142196210589	170.354001821091472
5	-4850.316	5.912626209773153	53.992906912940207
6	8031.468	0.564189583562615	10.479857114260399

Table II–5: Series Expansion Coefficients for Voigt Function

where the second expression means the real (\Re) part of the rational function of the complex variable $\zeta = a - iv$. The coefficients are given in Table II-5.

3. Doppler broadening is calculated with a statistical theory. For a Maxwell-Boltzmann distribution of thermal velocities (non-relativistic ideal Boltzmann gas) one obtains a Gauss profile with thermal Doppler width

$$\Delta \lambda_{\rm G} = \Delta \lambda_{th} = \lambda_{\rm o} \frac{\sqrt{2kT/m_{\beta}}}{c},\tag{II-33}$$

where m_{β} is the radiating particle mass. If, additionally, classical microturbulence (velocity = ξ) is taken into account, one obtains a Gauss profile with Doppler width

$$\Delta \lambda_{\rm G} = \Delta \lambda_D = \lambda_{\rm o} \frac{\sqrt{2kT/m_{\beta} + \xi^2}}{c}.$$
 (II-34)

The statistical theory of thermal Doppler line broadening breaks down if λ_{\circ} is not small compared to the mean-free-path of particles between collisions (*i.e.*, radio waves and/or extremely high densities).

4. Radiation (natural) broadening of a line results from an excited state having a finite width or probability distribution due to the Heisenberg Uncertainty Principle. It approximately

yields a Lorentz profile with a damping constant

$$\gamma_{\rm rad} = \gamma_i + \gamma_j, \tag{II-35}$$

where γ_i and γ_j are the damping constants for the *i*-th and *j*-th levels. These damping constants are determined either quantum mechanically or by experiment.

- 5. Collisional broadening is caused by the interaction of radiating particles with surrounding matter. The E-fields of the perturbing particles affect the *level thicknesses* of the radiating, hence broadening the line. These collisional broadening events give rise to *Lorentzian* profiles. There are 4 types of collisional broadening events:
 - a) Linear Stark effect in a hydrogen-like particle due to a charged perturber.
 - b) Resonance interaction between two identical particles.
 - c) Quadratic Stark effect due to a charged perturber.
 - d) Van der Waals interaction between two particles of different species.
- 6. Rotational broadening, is a broadening of a spectral line due to the rotation of the emitting object. It must be taken into account if $v_{\rm rot} > \sim v_{\rm th}$, where $v_{\rm th}$ is the thermal velocity (i.e., in the Sun's photosphere, $v_{\rm th} \sim 10$ km/s, whereas $v_{\rm rot} = 2$ km/s \rightarrow hence the rotational velocity can be neglected).
 - a) Rotational broadening follows a Gaussian distribution similar to thermal Doppler broadening, except the rotation velocity replaces $\sqrt{2kT/m_{\beta}}$ in Equation II-33.

- transfer calculations for a stellar atmosphere. It can be included, however, at the end of an RT code when the emergent spectrum is being output to an external file, or (better yet), it can be included in a graphics package where an emergent synthetic line profile is convolved with the rotational velocity Gaussian.
- 7. Instrument broadening can further broaden a line in a spectrum due to attributes of the optical system (i.e., diffraction, filter characteristic, pixel size, etc.). One determines an instrument profile by taking a comparison spectrum of an emission lamp with "infinitely" sharp lines (that is, the natural broadening dominates atomic broadening mechanisms and the natural broadening is much less that the instrument profile). Generally an instrument profile is Gaussian in shape, but doesn't necessarily have to be.
 - a) When one speaks of spectral resolution, he/she is discussing the FWHM of the instrument profile \Longrightarrow high resolution spectra have $\Delta\lambda_{1/2}$ (instrument) < 0.1Å, whereas low resolution spectra have $\Delta\lambda_{1/2}$ (instrument) > 1Å.
 - b) Instrumental broadening should **never** be included anywhere in a RT or stellar atmospheres code. Instead, it should be taken account in a graphics package when comparing synthetic to observed spectra.
- 8. Beside the above mentioned broadening mechanisms, there are other processes that can affect a line profile. Magnetic fields ($Zeeman\ effect$) and e^- interactions with nucleus ($hyperfine\ structure$) are two such examples. We don't have time in this

course to discuss these and other topics of this nature. If you have interest in these topics, see *Radiative Processes in Astro-* physics by Rybicki & Lightman (1979, Wiley Publishing, p256-259.

9. You now have a good understanding of the mechanisms that lead to line broadening. A common practice among observers is to plot a line profile in velocity space instead of wavelength (or frequency) space, as though implying that each wavelength point directly maps into a real velocity. As you now know, this analysis technique is invalid for optically thick lines since broadening mechanisms other than Gaussian velocity fields dominate. Observers tend to do this quite often for Balmer lines, which generally are optically thick. Keep this in mind when reading such papers.

H. The Hertzsprung-Russell Diagram

- 1. In the early 1900s, 2 astronomers found peculiar groupings of stars when they plotted their absolute magnitude to their (B V) colors (Hertzsprung) or spectral type (Russell)
 - ⇒ the Hertzsprung-Russell (HR) Diagram (see Figure II-9).
 - a) Main sequence stars ($\sim 90\%$ of all stars are of this type).
 - b) Giant stars (most of them red in color).
 - c) Supergiant stars (very luminous, hence large).
 - d) White dwarf stars (very faint, hence small).
- 2. When plotting the HR diagram for a star cluster, the stars are virtually at the same distance, hence differences in *observed*

Figure II–9: The Hertzsprung-Russell Diagram.

brightness corresponds to actual luminosity differences (and not distance differences).

- a) The shape of an HR diagram for a star cluster gives the age of the star cluster.
- b) The main sequence turn-off point is a very precise gage of the cluster's age \Longrightarrow the point at which a main sequence star exhausts its supply of hydrogen in its core.
- **3.** HR diagrams come in 2 types:
 - a) Observed HR diagrams, absolute magnitude (M_V) , or apparent magnitude (V) for clusters, versus color index (B-V) or spectral type.
 - i) The **color index** is the magnitude difference between 2 different filter measurements (see Table I-1). The color index, or *color*, is related to the temperature of the star.

- ii) For very hot stars (e.g., O stars), (U B) gives the most accurate temperature measurements. These stars appear bluish.
- iii) For very cool stars (e.g., M stars), (V R) or (R I) gives the most accurate temperatures. These stars appear reddish.
- iv) For every other star, (B V) gives the most accurate temperatures.
- v) Faint, bluish stars are on the lower left side of an HR diagram, and bright, reddish stars are on the upper right.
- b) Theoretical HR diagrams plot luminosity (L/L_{\odot}) versus effective temperature $(T_{\rm eff})$ of the star.
 - i) Eddington, through the process of radiative diffusion, showed that $L \propto M^4$ on the main sequence, or

$$\frac{L}{L_{\odot}} = \left(\frac{M}{M_{\odot}}\right)^4. \tag{II-36}$$

ii) Since the time that a star spends on the main sequence depends on the amount of fuel the star has (M) divided by the rate at which it burns that fuel (L), the main sequence lifetime of a star is $t_{\text{life}} \propto M/L$ or M^{-3} , hence

$$t_{\rm life} = \left(\frac{M_{\odot}}{M}\right)^3 \times 10^{10} \text{ years.}$$
 (II-37)

iii) The y-axis goes from low (lower portion) to high luminosity (upper portion).

iv) The x-axis goes from hotter temperatures (left side) to lower temperatures (right side).